16th Australasian Fluid Mechanics Conference
Crown Plaza, Gold Coast, Australia
2-7 December 2007

Numerical Investigation of Shallow Depth Sloshing Absorbers for Structural Control

A. P. Marsh[1], M. Prakash[2], S. E. Semercigil[1] and Ö. F. Turan[1]

[1]School of Architectural, Civil and Mechanical Engineering
Victoria University, Melbourne, Victoria, 3011 AUSTRALIA

[2]CSIRO Mathematical and Information Sciences
CSIRO, Clayton, Victoria, 3168 AUSTRALIA

Abstract

A liquid sloshing absorber consists of a container, partially filled with liquid. The absorber is attached to the structure to be controlled, and relies on the structure's motion to excite the liquid. Consequently, a sloshing wave is produced at the liquid free surface within the absorber, possessing energy dissipative qualities. The behaviour of liquid sloshing absorbers has been well documented, although their use in structural control applications has attracted considerably less attention.

Generally it is accepted that sloshing absorbers with lower liquid levels are more effective energy dissipaters than those with higher levels, although there has not yet been a study to reveal an 'optimum' design mechanism. The main limitation of numerically modelling such circumstances is the inherent complexity in the free surface behaviour, predictions of which are limited when using grid-based modelling techniques. Considering such limitations, Smoothed Particle Hydrodynamics (SPH) is used in this study to model a 2-dimensional rectangular liquid sloshing absorber. SPH is a Lagrangian method of solving the equations of fluid flow that is suitable to model liquid sloshing due its grid-free nature, and inherent ability to model complex free surface behaviour.

The primary objective of this paper is to numerically demonstrate the effect of tuning a container's width, to complement previous work [6] on the effect of liquid depth. This study is in an attempt to reveal geometry that enables both effective energy transfer to sloshing liquid and to dissipate this energy quickly.

Introduction

Sloshing is the oscillation of a liquid within a partially full container. Efforts are usually directed towards suppression, due to the damaging effects it can impose. Sloshing has an inherent ability to dissipate large amounts of energy via shearing of the fluid. For this reason, it is possible to employ liquid sloshing as an energy sink in structural control applications, providing protection for structures exposed to excessive levels of vibration.

Liquid sloshing in rectangular tanks has long been an area of study. However, the analysis of complex free surface behaviour exhibited by such a system has limited the numerical prediction attempts. Such behaviour is of great interest in structural control due to its intrinsic ability to dissipate large amounts of kinetic energy quickly.

Studies on the implementation of liquid sloshing as a structural control mechanism can be found in the literature [1-6], although the effectiveness of shallow liquid levels (where the liquid depth is a small faction of the container width) has not been studied as extensively. Numerical modeling of such circumstances has been limited due to the inherent complex free surface behaviour exhibited.

Due to complex free surface behaviour Smoothed Particle Hydrodynamics (SPH) is used in this study to model 2-dimensional rectangular liquid sloshing absorbers. SPH is a Lagrangian method of solving the equations of fluid flow that is suitable to model liquid sloshing due to its grid-free nature, and inherent ability to capture complex free surface behaviour [7]. SPH has been successfully applied to a wide range of industrial fluid flow applications [8-12].

In this paper, transfer and dissipation of kinetic energy within a rectangular tank has been investigated while varying liquid depth, and container width. This objective is, hence, an attempt to reveal liquid depth and absorber geometry that optimises energy transfer and dissipation.

Methodology

The SPH computer code used in this study has been developed by CSIRO Mathematical and Information Sciences Division. SPH is a particle-based method of modelling fluid flows. The fluid being modelled is discretized into fluid elements, the properties of which are attributed to their centres. SPH is a Langrangian continuum method used for solving systems of partial differential equations. The method works by tracking particles and approximating them as moving interpolation points.

The interpolated value of any particle property A at position r is approximated using the information from nearby particles lying within a radius of 2h from the particle of interest, and is governed by Equation 1.

$$A(r) = \sum_b m_b \frac{A_b}{\rho_b} W(r - r_b, h) \qquad (1)$$

where: W is an interpolation kernel
h is the interpolation length
m_b is the mass of particle j
r_b is the position of particle j
ρ_b is the density of particle j
A(r) is property A of a particle at position r

The SPH continuity equation is,

$$\frac{d\rho_a}{dt} = -\sum_b m_b (v_a - v_b) \bullet W_{ab} \tag{2}$$

where $W_{ab} = W(r_{ab}, h)$ and is evaluated for the distance $|r_{ab}|$. r_{ab} is the position vector from particle 'b' to particle 'a' and is equal to $r_a - r_b$.

The SPH momentum equation is,

$$\frac{dv_a}{dt} = -\sum m_b \left[\left(\frac{P_b}{\rho_b^2} + \frac{P_a}{\rho_a^2} \right) - \frac{\zeta}{\rho_a \rho_b} \frac{4\mu_a \mu_b}{(\mu_a + \mu_b)} \frac{v_{ab} r_{ab}}{(r_{ab}^2 + \eta^2)} \right] \nabla_a W_{ab} + g \tag{3}$$

where P_a and μ_a are the pressure and viscosity of particle 'a', the same applies for particle 'b'. $v_{ab} = v_a - v_b$, the velocity of particle 'b' subtracted from the velocity of particle 'a'. ζ is a factor having a theoretical value of 4. η is a parameter used to smooth out the singularity at $r_{ab} = 0$, and g is the gravitational acceleration.

The SPH code developed by CSIRO uses a compressible method for determining the fluid pressure. It is operated near the incompressible limit by selecting a speed of sound that is much larger than the velocity scale expected in the fluid flow.

The equation of states that governs the relationship between particle density and fluid pressure is,

$$P = P_0 \left[\left(\frac{\rho}{\rho_0} \right)^{\gamma} - 1 \right] \tag{4}$$

where P_0 is the magnitude of pressure and ρ_0 is the reference density. The pressure the equation of state solves for P is then used in the SPH momentum equation governing the particle motion. For water, $\gamma = 7$ is generally used. More information on SPH can be found in [13].

A rigid container 400mm high, of varying width (W), and varying liquid depth (L) is subjected to a horizontal sinusoidal displacement function of pure translation with amplitude of 50mm and a frequency of 1.4 Hz for one complete cycle. The numerical model is shown in Figure 1 along with the excitation shown in Figure 2. The fluid being modelled is water with a density of 1000 kg/m^3 and viscosity of 0.001 kg/m.s. A particle represents a 0.8mm x 0.8mm area of water within the container.

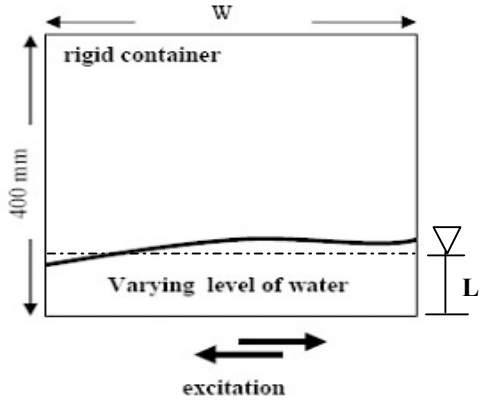

Figure 1 2-D numerical model of the sloshing container.

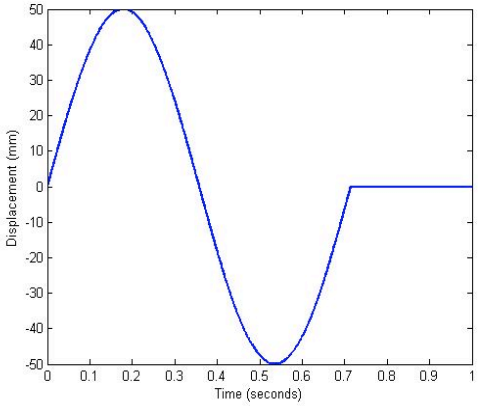

Figure 2 Base excitation history.

The fluid within the container is left to settle under gravity for a period of one second, after which it is subjected to the sinusoidal excitation. The fluid is then allowed to respond naturally to the excitation within the container. The total simulation time is 20 seconds. Due to the base excitation imposing increasing amounts of kinetic energy to the fluid as its mass increases, all analysis has been undertaken on a per unit mass basis.

Results

An efficient absorber needs to transfer a substantial amount of energy from the structure in which it is employed, to the working fluid. This energy is then to be dissipated as quickly as possible. The primary means of energy dissipation is the shearing of the fluid. Energy dissipation is enhanced as the velocity gradients in the flow become steeper. Two events produce steep velocity gradients in a sloshing liquid, namely wave-to-wave and wave-to-wall interactions. In general, wave-to-wave interactions seem to be more effective.

Two waveforms, travelling and standing, can exist in a sloshing liquid. A travelling wave is the principal waveform found in liquid levels of and below 20mm depth in a 400mm wide container. In a container of the same width, standing waves are observed to be the governing waveform in liquid levels of 40mm and more. A travelling wave is capable of producing both type of interactions mentioned above, whereas standing waves produce only wave-to-wall interactions.

Histories of the kinetic energy per unit mass for all cases in a container of 400mm width, are shown in Figure 3. Such histories show the sum of kinetic energy of all fluid particles within the absorber. Peaks in the kinetic energy histories correspond to high particle velocities, when the surface shape is relatively flat. Troughs in the kinetic energy histories are observed when the fluid is close to largest surface deformation, corresponding to a high potential energy.

In cases where periodic behaviour is observed in the history of kinetic energy, two wave-to-wall interactions take place per sloshing cycle, producing two peaks and two troughs. This results in the frequency of liquid sloshing being half of that observed in the kinetic energy histories. Figures 3(a) to 3(h) correspond to the liquid depths of 5mm, 10mm, 15mm, 20mm, 40mm, 60mm, 80mm and 100mm, in descending order. Positions indicated with a red arrow indicate the point of maximum kinetic energy; text indicating the corresponding magnitude.

The liquid levels in Figures 3(a) through to 3(d) produce an irregular dissipation history, with a steeper rate of dissipation relative to deeper liquid levels. As the water level gets deeper, a quasi-periodic behaviour begins to emerge, the distinct transition is noticeable from Figures 3(d) to 3(f). As this quasi-periodic behaviour becomes more dominant, the energy dissipation rate becomes more gradual. The physical significance of this transition is the change of the principal waveform from travelling to standing.

The shallowest case of 5mm depth shown in Figure 3(a) dissipates its energy the quickest. The deepest case of 100mm dissipates its energy the slowest. Between the depths of 5mm and 20mm the overall time taken to dissipate the total energy increases slightly, yet there is an approximately 5 fold increase in the amount of energy transferred from the excitation to the working fluid. The case of 20mm liquid depth is the deepest liquid level that possesses a dominant travelling waveform, and its inherent effective energy dissipation characteristics.

A comparison of the 20mm and 100mm liquid depth cases, simulated in a container width of 400mm is shown in Figure 4. The left hand column represents 20mm liquid depth, the right hand column 100mm liquid depth. The sliding scale at the bottom of these figures indicates particle velocity, the point in time at which this occurs is shown in the top right of the frame. Figure 4(a) shows the development of the first travelling wave in the 20mm liquid depth simulation. The wave motion is from left to right corresponding to that of the excitation.

The probability distribution of this case (kinetic energy history of which is shown in Figure 3(d)) is shown in Figure 4(c). The probability distribution shows that the fluid spends most of its time at very low kinetic energy levels. Almost half of the simulation time is spent within the first bar, corresponding to the lowest possible energy level. A very little amount of mid-level energy is observed, resulting in a high rate of dissipation.

In contrast to the travelling waveform development observed in the 20mm liquid depth case, Figure 4(b) shows a standing wave in a liquid depth of 100mm producing a wave-to-wall interaction. This interaction results in a large portion of the fluid situated at a high potential, and corresponds to the first trough after the maximum kinetic energy is observed in Figure 3(h). The periodic oscillation in the kinetic energy history of this case is due to the predominant standing waveform. The probability distribution of the 100mm liquid depth case is shown in Figure 4(d). A significant amount of mid-level energy is observed; most of the simulation is spent in a mid-level kinetic energy band corresponding to a more gradual rate of energy decay.

The maximum kinetic energy transferred from the moving base excitation to the fluid for varying liquid depths in a container of 400mm width, is shown in Figure 5. The behaviour shown indicates that there is more energy being introduced into the system on a per unit mass basis as the liquid level increases.

Figure 6 has the summary of the settling time analysis of varying liquid depths in a 400mm wide container. The settling time is defined as the time taken for the kinetic energy within the fluid to reach a certain percentage of the maximum amount introduced into the system. At the lower liquid levels of 5mm, 10mm, 15mm and 20mm the settling time is relatively low in comparison with the higher liquid levels. As expected, there is not a significant difference in settling time between these depths, where travelling waves are predominant. At the liquid depth of 40mm there is a dramatic increase in settling time magnitude. This step change is due to the transition from travelling wave to standing wave. At the deep liquid levels of 80mm and 100mm only standing waves can be seen.

Histories of the kinetic energy for all cases simulated with a constant liquid depth of 20mm are shown in Figure 7. 20mm liquid depth was chosen for tuning analysis due to being the highest liquid depth that possesses a predominant travelling waveform and, therefore, its energy dissipative qualities. Figures 7(a) to 7(h) correspond to container widths of 25mm, 50mm, 75mm, 100mm, 125mm, 150mm, 200mm and 400mm, in descending order. As in Figure 3, a red arrow indicates the point of maximum kinetic energy and its corresponding magnitude.

All cases, with the exceptions of 25mm and 400mm container widths, have a noticeable periodic behaviour within their dissipation histories. The overall time taken to dissipate the total energy increases slightly between the container widths of 25mm and 200mm, a significant increase is seen between 200mm and 400mm container widths. Reducing the container width increases the number of wave-to-wall interactions that occur within a given time period, and the dissipation becomes faster as a result of this.

The maximum kinetic energy transferred from the excitation to the fluid for varying container widths, but for the constant liquid depth of 20mm is shown in Figure 8. The data indicates that the optimum energy transfer condition occurs at the 125mm container width. A summary of the settling time analysis of varying container width, employing a liquid depth of 20mm is presented in Figure 9. The general trend shows that the settling time increases as the container width increases, due to decreasing number of wave-to-wall interactions.

Conclusions

The primary form of energy dissipation in a sloshing liquid is shearing of the fluid. Shear stress is increased through providing steep velocity gradients. Two types of interactions are responsible for producing steep velocity gradients, those being wave-to-wave and wave-to-wall interactions. Travelling waves have the ability to produce both of these interactions, whereas standing waves only produce wave-to-wall interactions.

Travelling waves are generated in shallow liquid levels of around 20mm and lower, in a 400mm wide rectangular container. As the liquid level increases, a transition to a standing waveform occurs. This transition produces undesirable energy dissipative characteristics resulting in an increase in settling times. Hence, a liquid depth higher than 20mm in a 400mm wide container is not recommended. An optimum energy transfer condition exists when varying container width, for a constant liquid depth of 20mm. This optimum condition occurs at a width of 125mm. Therefore, an ideal rectangular absorber would employ a liquid depth of 20mm in a container of 125mm width.

Observations stated here should not be taken as the best possible design, rather a result of limited case studies conducted numerically. Experimental verification of the numerical predictions is underway.

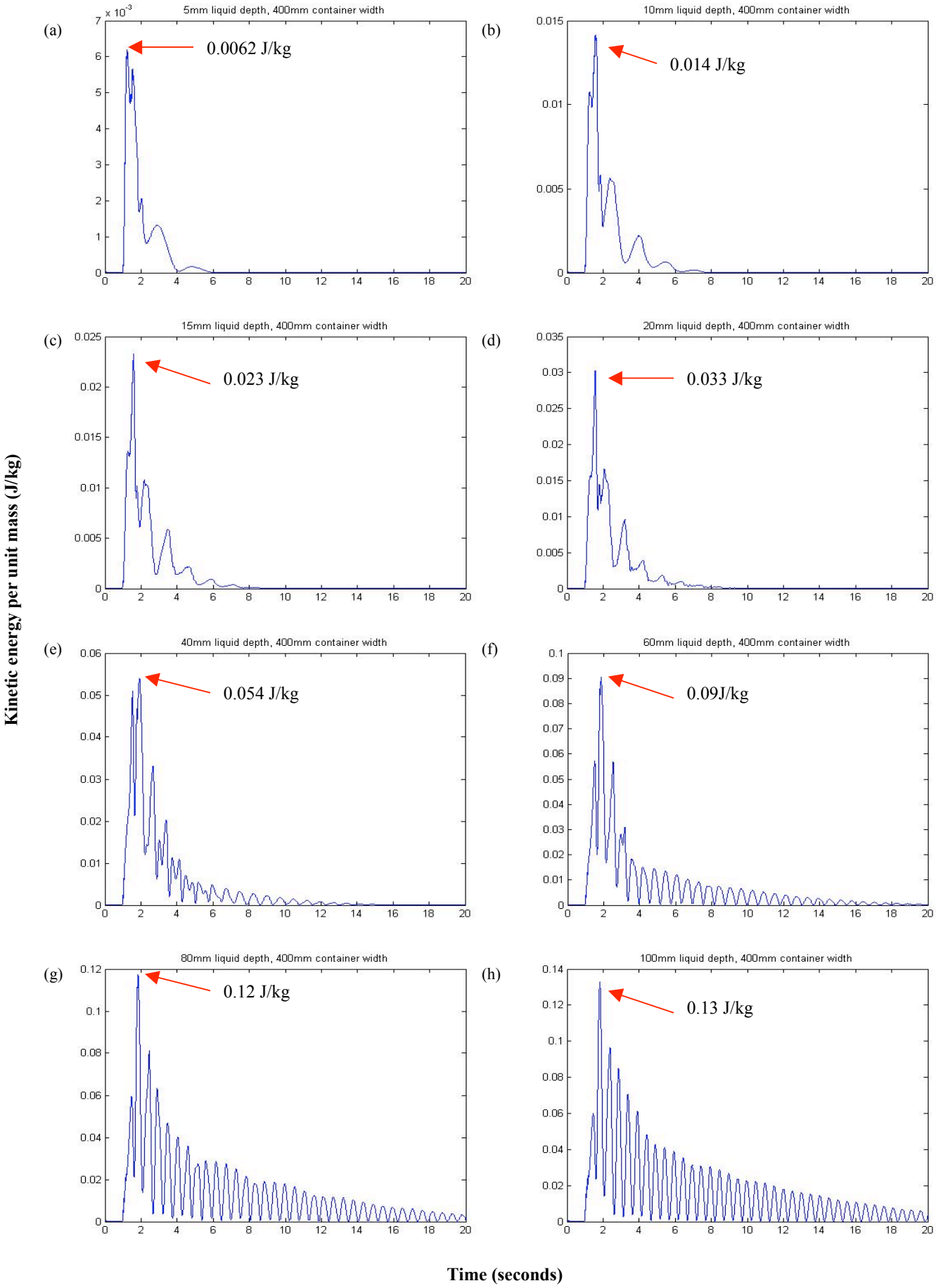

Figure 3 Kinetic energy dissipation histories for different water depths (indicated on top of each frame) with a constant container width of 400mm.

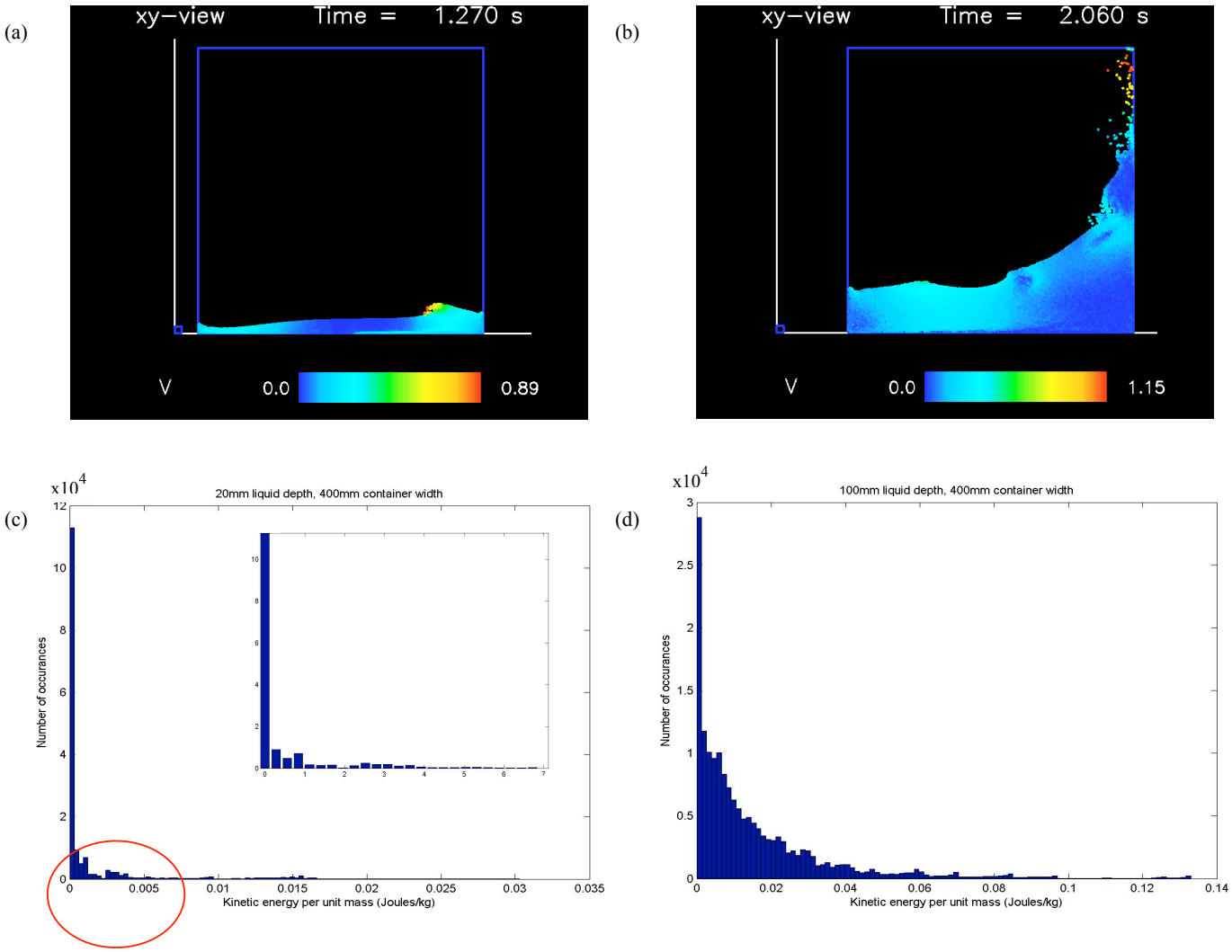

Figure 4 Comparison of 20mm and 100mm liquid depth in a 400mm wide container. Left column shows 20mm liquid depth, right column shows 100mm liquid depth. (a) and (b) show still frames at instants of interest from simulations. (c) and (d) show probability distributions of the kinetic energy histories.

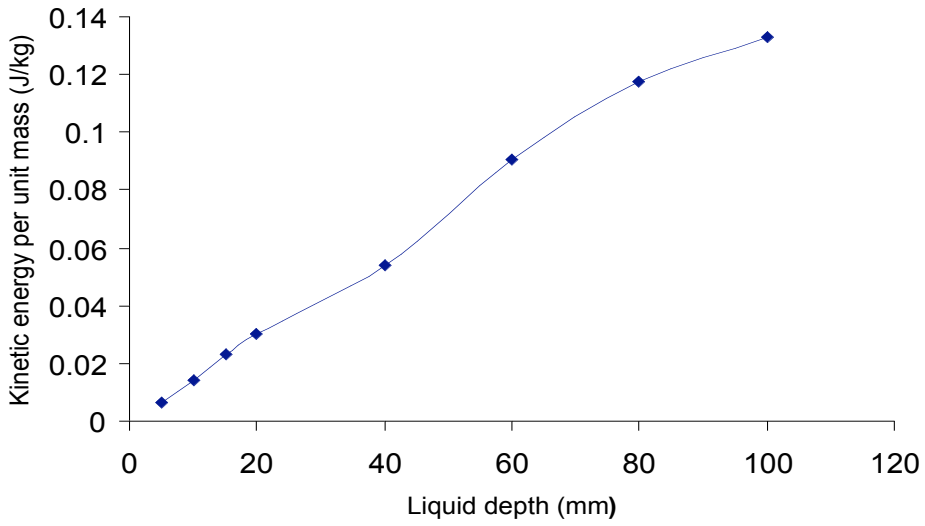

Figure 5 Variation of maximum kinetic energy transfer for different water depths. For the constant container width of 400mm

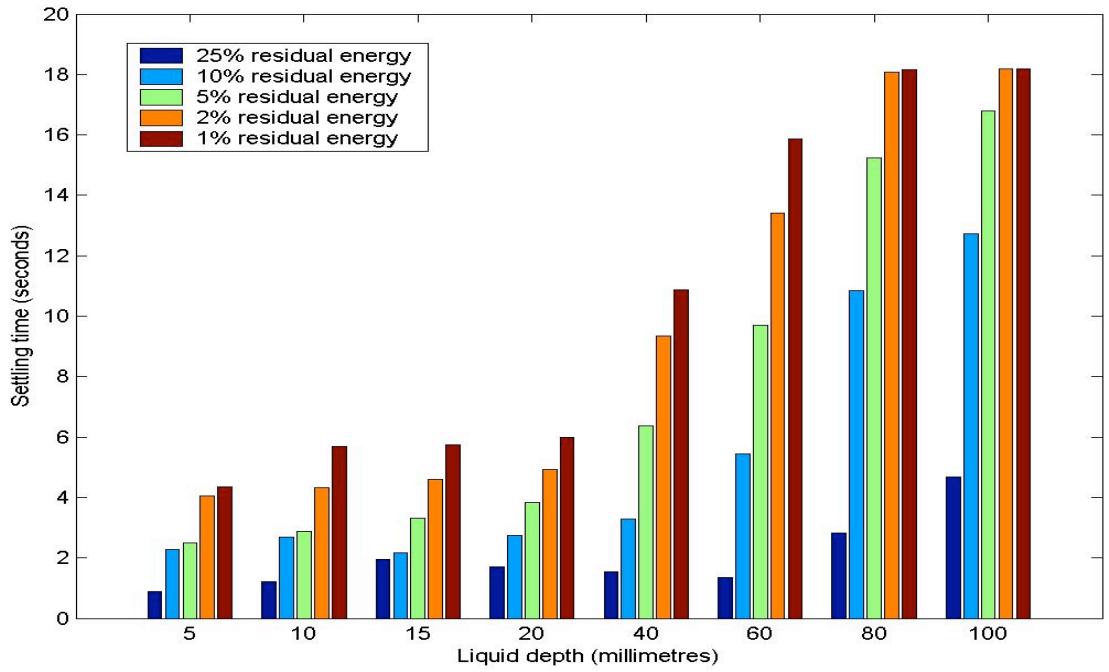

Figure 6 A summary of settling times for different water depths for a constant container width of 400mm.

References

[1] Modi, V. J. & Seto, V. L., Suppression of Flow Induced Oscillations Using Sloshing Liquid Dampers: Analysis and Experiments, *J. of Wind Eng. & Ind. Aerodyn.*, **67&68**, 1997, 611-625.

[2] Shankar, K. & Balendra, T., Application of the Energy Flow Method to Vibration Control of Buildings with Multiple Tuned Liquid Dampers, *J. of Wind Eng. & Ind. Aerodyn.*, **90**, 2002, 1893-1906.

[3] Li, S., J., Li, G., Q., Tang, J. & Li, Q., Shallow Rectangular TLD for Structural Control Implementation, Applied Acoustics, **63**, 2002, 1125-1135.

[4] Anderson, J. G., Semercigil, S.E. & Turan, O. F., A Standing-Wave Type Sloshing Absorber to Control Transient Oscillations, *Journal of Sound and Vibration*, **232**, 2000, 838-856.

[5] Banjeri, P., Murudi, M., Shah, A., H. & Popplewell, N., Tuned Liquid Dampers for Controlling Earthquake Response of Structures, Earthquake Engineering. *Structural Dynamics*, **29**, 2000, 587-602.

[6] Guzel, B., Prakash, M., Semercigil, S.E. & Turan, Ö.F., Energy Dissipation with Sloshing for Absorber Design, *International Mechanical Engineering Congress and Exposition*. IMECE2005-79838.

[7] Monaghan, J.J., Smoothed particle hydrodynamics. *Ann. Rev. Astron. Astrophys.*, **30**, 1992, 543-574.

[8] Prakash, M., Cleary, P.W., Grandfield, J., Rohan, P. & Nguyen, V., Optimisation of ingot casting wheel design using SPH simulations. *Progress in Computational Fluid Dynamics*, **7(2-4)**. Call No: 2264. 2007.

[9] Cleary, P.W., Prakash, M., Ha, J., Stokes, N. & Scott, C., Smooth particle hydrodynamics: status and future potential. *Progress in Computational Fluid Dynamics*, **7**, 2007, 70-90.

[10] Prakash, M., Cleary, P.W., Ha, J., Noui-Mehidi, M.N., Blackburn, H.M. & Brooks, G., Simulation of suspension of solids in a liquid in a mixing tank using SPH and comparison with physical modelling experiments. *Progress in Computational Fluid Dynamics*, **7**, 2007, 91-100.

[11] Gomme, P.T., Prakash, M., Hunt, B., Stokes, N., Cleary, P., Tatford, O.C. & Bertolini, J., Effect of lobe pumping on human albumin: development of a lobe pump simulator using smoothed particle hydrodynamics. *Biotechnology and Applied Biochemistry*, **43**, 2006, 113-120.

[12] Cleary, P.W., Ha, J., Prakash, M., & Nguyen, T., 3D SPH Flow Predictions and Validation for High Pressure Die Casting of Automotive Components. *Applied Mathematical Modelling*, **30,** 2006, 1406-1427.

[13] Cleary, P.W., and Praksah, M., Discrete-Element Modelling and Smoothed Particle Hydrodynamics: Potential in the Environmental Sciences, *Phil. Trans. R. Soc. Lond.*, **362**, 2004, 2003-2030.

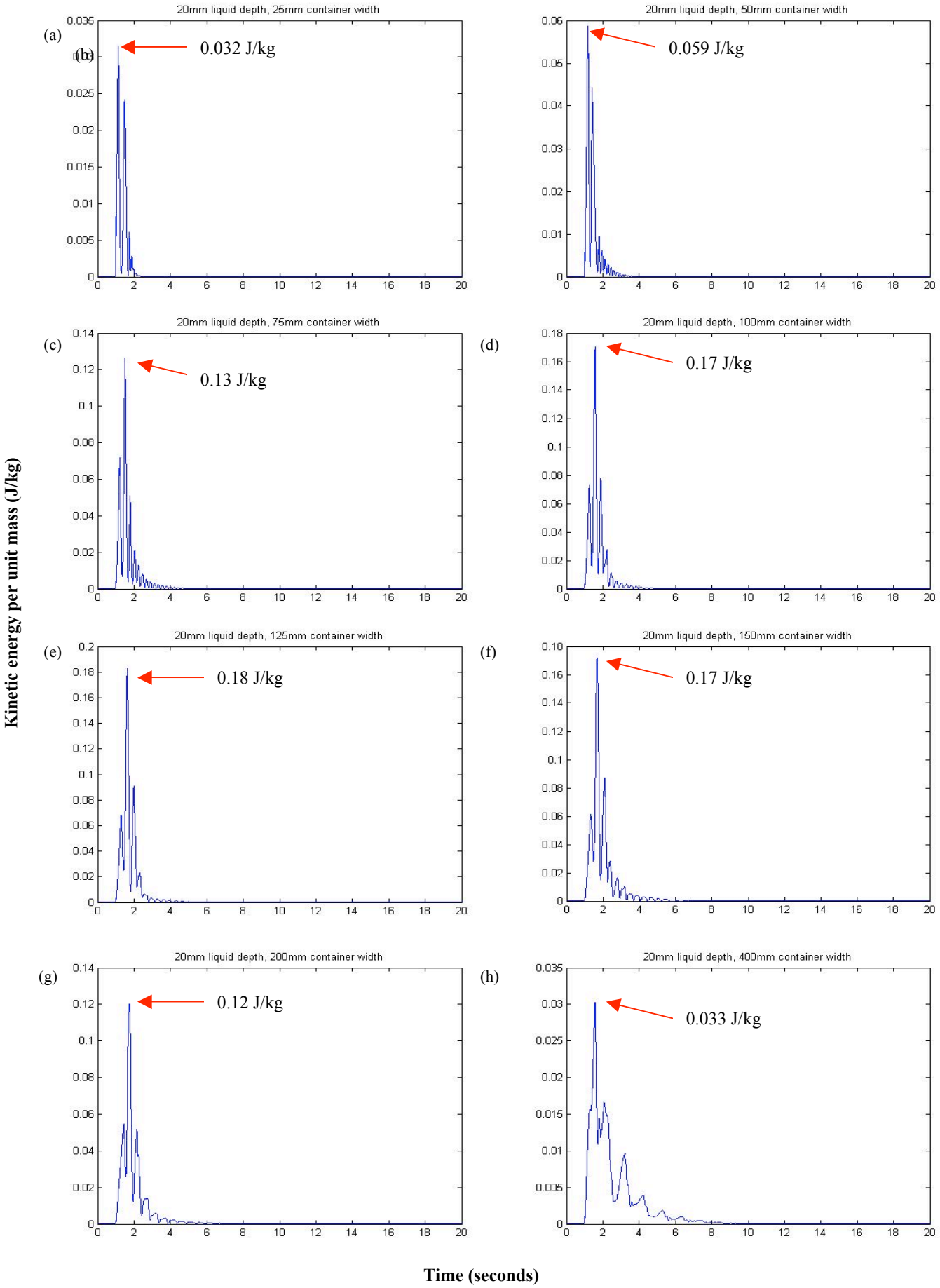

Figure 7 Kinetic energy dissipation histories for different container widths (indicated on top of each frame) with a constant depth of 20mm

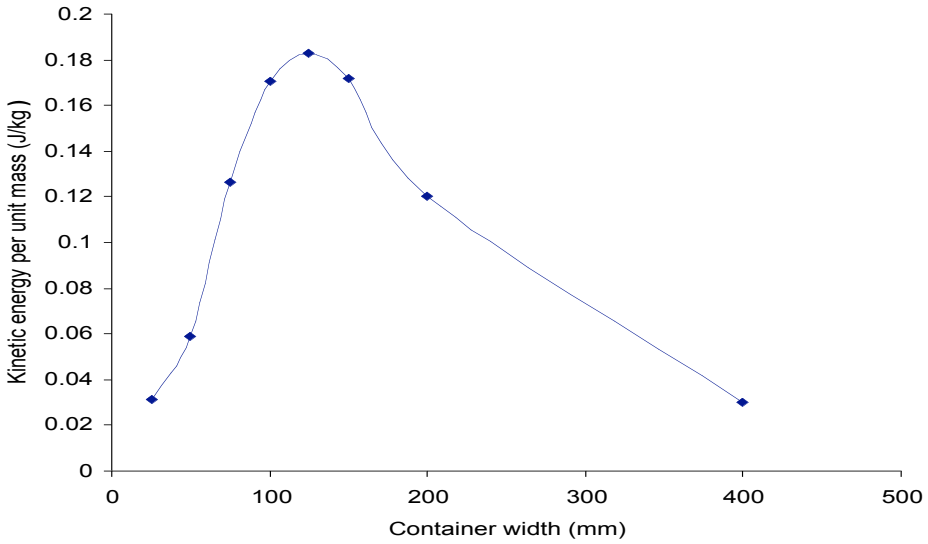

Figure 8 Kinetic energy transfer of different container widths for constant water depth of 20mm.

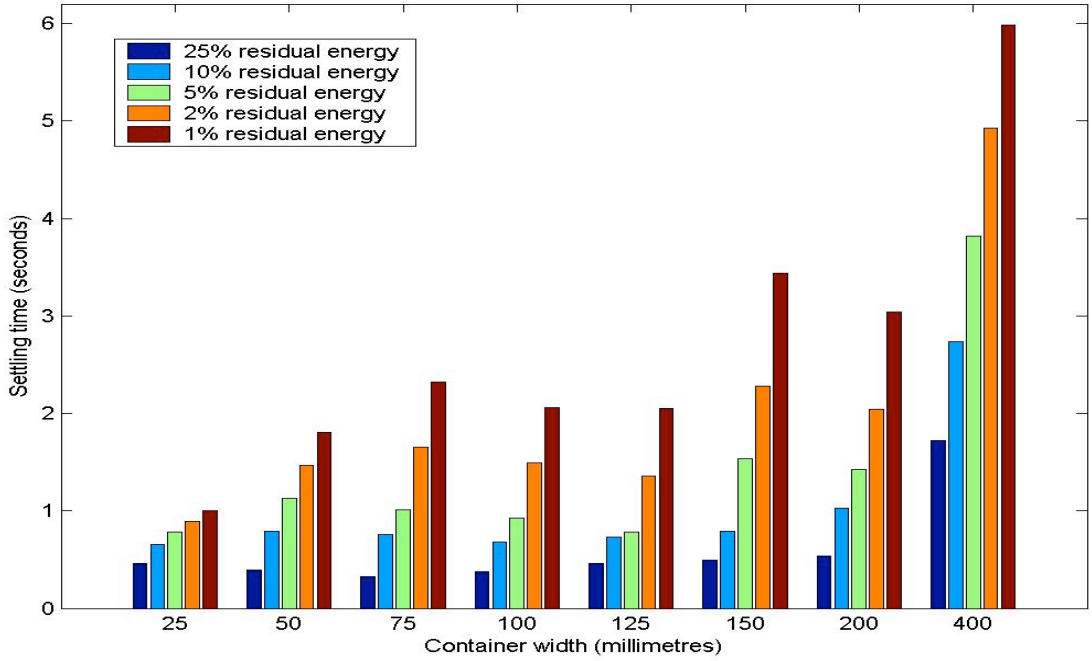

Figure 9 A summary of settling times for different container widths for constant liquid depth of 20mm.